

Colloid-Imprinted Carbons as Templates for the Nanocasting Synthesis of Mesoporous ZSM-5 Zeolite

Seong-Su Kim, Jainisha Shah, and Thomas J. Pinnavaia*

Department of Chemistry, Michigan State University, East Lansing, Michigan 48824

Received November 27, 2002. Revised Manuscript Received February 11, 2003

Colloid-imprinted carbons (CIC) with average pore sizes of 12, 22, 45, and 85 nm have been used as templates for the nanocasting of ZSM-5 zeolite with spherical domain sizes comparable to the pore sizes of the CIC template. The size and shape fidelity of the CIC-nanocasted zeolite allows one to control both the external surface area (16–127 m²/g) and the interparticle mesopore volume (0.05–1.19 cm³/g) through a rational choice of the template pore size. This flexibility in tailoring the particle textural properties makes it possible to optimize the catalytic properties of the zeolite for the conversion of molecules that are too large to penetrate the framework micropores and constrained to reacting only at active sites on the external particle surfaces. Conversely, for small molecule conversions within the framework micropores, the nanocasting method allows uniform tailoring of the diffusion path length to optimize reactivity or selectivity.

Introduction

Zeolites and zeo-type phases are used extensively to catalyze a number of chemical reactions in refinery and petrochemical processing.¹ Owing to their microporous channel structures (pore sizes <2 nm) and monolithic particle morphology, these materials are subject to diffusional limitations that restrict substrate accessibility to active sites on the interior surfaces. Several approaches are currently being investigated as possible solutions to this limitation. For instance, new generations of mesostructured aluminosilicates, such as those represented by the M41 S family of materials,² are being developed with pore sizes >2 nm. Also, the diffusion length into the framework structure of conventional zeolite crystals is being reduced through the introduction of extraframework mesoporosity using various postsynthesis treatment methods.^{3–6} In addition, mesopores have been introduced in zeolite crystals by occluding small (12 or 18 nm) nanosized carbon particles or macromolecules into the crystals during synthesis and subsequently removing them through oxidation.^{7–9}

As an alternative to forming new mesostructures or to creating mesoporosity in zeolitic crystals, another

possibility is to decrease the crystal size of a zeolite, thereby increasing the external surface area and reducing the diffusion path length. Nanosized zeolites have received much attention in catalytic applications including fluid catalytic cracking (FCC), hydrocracking of gas oil, hydroxylation of phenol, and the hydration of cyclohexene to cyclohexanol.^{10–14} For ZSM-5 with crystal sizes of 30–70 nm, for instance, an increase in toluene conversion and selectivity to cresol was observed in comparison to that of conventional ZSM-5 powders.¹⁵ Also, ZSM-5 with an average particle size of 30 nm exhibited reduced deactivation through coke formation in the catalytic aromatization of ethylene.¹⁶

Several synthetic routes have been reported for the preparation of nanosized (<50 nm) zeolite crystals.¹⁷ For instance, ZSM-5 zeolite with crystal sizes of 30–50 nm¹⁶ and 15–30 nm¹⁸ have been realized through careful control of the reaction stoichiometry and the crystallization time and temperature. Efforts to prepare ZSM-5 particles with an average size smaller than 8 nm have resulted in the formation of X-ray amorphous products.¹⁹

* To whom correspondence should be addressed via E-mail: pinnavaia@cem.msu.edu.

(1) Baerlocher, C. H.; Meier, W. M.; Olson, D. H. *Atlas of Zeolite Framework Types*; 5th ed.; Elsevier Science: Amsterdam, 2001.

(2) Kresge, C. T.; Leonowicz, M. E.; Roth, W. J.; Vartuli, J. C.; Beck, J. S. *Nature* **1992**, *359*, 710–712.

(3) Ogura, M.; Shinomiya, S. Y.; Tateno, J.; Nara, Y.; Kikuchi, E.; Matsukata, H. *Chem. Lett.* **2000**, 882–883.

(4) Groen, J. C.; Perez-Ramirez, J.; Peffer, L. A. A. *Chem. Lett.* **2002**, 94–95.

(5) Suzuki, T.; Okuhara, T. *Microporous Mesoporous Mater.* **2001**, *43*, 83–89.

(6) Scherzer, J. *ACS Symp. Ser.* **1984**, *248*, 157.

(7) Jacobsen, C. J. H.; Madsen, C.; Houzvicka, J.; Schmidt, I.; Carlsson, A. *J. Am. Chem. Soc.* **2000**, *122*, 7116–7117.

(8) Schmidt, I.; Boisen, A.; Gustavsson, E.; Stahl, K.; Pehrson, S.; Dahl, S.; Carlsson, A.; Jacobsen, C. J. H. *Chem. Mater.* **2001**, *13*, 4416–4418.

(9) Zhang, B. J.; Davis, S. A.; Mann, S. *Chem. Mater.* **2002**, *14*, 1369–1375.

(10) Van der pol, A. J. H. P.; Verduyn, A. J.; Van Hoff, J. H. C. *Appl. Catal., A* **1992**, *92*, 113–130.

(11) Rajagopalan, K.; Peters, A. W.; Edwards, G. C. *Appl. Catal.* **1986**, *23*, 69–99.

(12) Cambor, M. A.; Corma, A.; Martinez, A.; Mocholi, F. A.; Pariente, J. P. *Appl. Catal.* **1989**, *55*, 65–74.

(13) Cambor, M. A.; Corma, A.; Martinez, A.; Martinez-Soria, V.; Valencia, S. *J. Catal.* **1998**, *179*, 537–547.

(14) Notari, Y. *Innovation in Zeolite Materials Science*; Elsevier Science Publishers: Amsterdam, 1987; Vol. 37.

(15) Vogel, B.; Schneider, C.; Klemm, E. *Catal. Lett.* **2002**, *79*, 107–112.

(16) Yamamura, M.; Chaki, K.; Wakatsuki, T.; Okado, H.; Fujimoto, K. *Zeolites* **1994**, *14*, 643–649.

(17) Lovallo, M. C.; Tsapatsis, M. *Advanced Catalysts and Nanostructured Materials*; Academic Press: San Diego, 1996.

(18) Mintova, S.; Bein, T. *Adv. Mater.* **2001**, *13*, 1880–1883.

(19) Jacobs, P. A.; Derouane, E. G.; Weitkamp, J. *J. Chem. Soc. Chem. Commun.* **1981**, 591–593.

Recently, nanosized ZSM-5 crystals have been prepared by crystallizing the zeolite in the void spaces of a carbon black and then removing the carbon by combustion in air.²⁰ However, the resulting nanocrystal size distribution was very broad, as expected for a disordered carbon template. Mesoporous carbons with much more uniform pore size distributions can be formed through the carbon replication of mesostructured silicas^{21–24} and through the colloid imprinting of pitch.²⁵ In comparison to carbon blacks, these latter carbons should be much more suitable templating media for the “nanocasting”²⁶ of zeolite phases, in part, because the pore sizes are far more uniform.

In the present work we demonstrate for the first time the nanocasting synthesis of a zeolite (ZSM-5) with highly uniform crystal size distributions through the use of colloid-imprinted carbons (CIC)²⁵ as the crystal templating medium. These latter mesoporous carbons are made through the direct, low-cost, colloidal silica imprinting of pitch.

Experimental Section

Materials. Mesophase pitch (AR Grade MP-H) as the carbon source was obtained from Mitsubishi Chemicals. Aqueous colloidal suspensions of silica were obtained from Aldrich Chemicals and Nissan Chemicals. The trade names of the colloidal silicas and the corresponding manufacturer-specified average particle diameters were as follows: Ludox AS-30 (12 nm); Ludox AS-40 (22 nm); Snowtex-OL (45 nm); and Snowtex-ZL (85 nm). Tetraethyl orthosilicate (TEOS), tetrapropylammonium hydroxide, and aluminum isopropoxide used in the nanocasting synthesis of nanosized ZSM-5 zeolite were purchased from Aldrich and used without further purification.

Synthesis of CIC Carbons. Colloid-imprinted carbons (CICs) were prepared through the imprinting of pitch with colloidal silica according to the general procedure reported by Li and Jaroniec.²⁵ A silica to pitch weight ratio between 0.8 and 1.6 was found to be effective in forming the imprinted carbon template. The preparation of a CIC using Snowtex-ZL as the imprinting agent serves as a typical example. A 15.0 g portion of ground mesophase pitch was dispersed in 150 g of ethanol. Then, 60.0 g of Snowtex-ZL colloidal suspension (40 wt % silica) was added, and the resulting mixture was stirred overnight at 50 °C. The resulting mixture was transferred to an open, wide-mouth, plastic bottle and kept at 50 °C to allow the solvent to evaporate under stirring. The air-dried mixture was further dried at 285 °C under nitrogen flow for 1 h. Then, the dried colloidal silica–pitch composite was carbonized at 900 °C for 2 h under nitrogen. The resulting silica–carbon composite was washed twice with 10 wt % hydrofluoric acid at room temperature to remove the silica template. The CIC carbons formed in this way were denoted as CIC-13, CIC-24, CIC-45, and CIC-90, where the number indicates the diameter of the imprinted carbon in nanometers, as determined by nitrogen adsorption.

Nanocasting Synthesis of ZSM-5. In a typical synthesis of nanosized ZSM-5 the CIC was impregnated to incipient wetness with a clear solution of tetrapropylammonium hy-

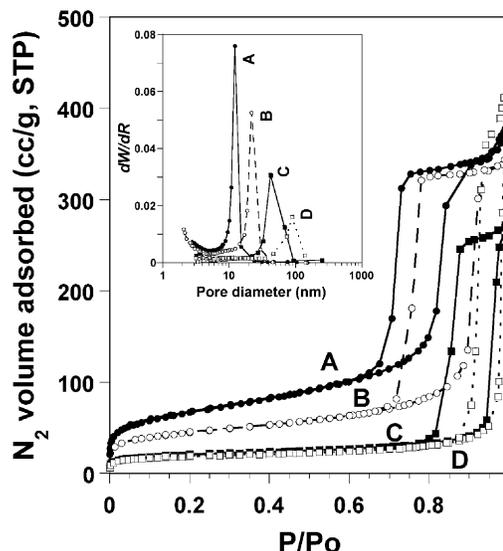


Figure 1. Nitrogen adsorption–desorption isotherms for mesoporous CIC carbons formed through imprinting pitch with colloidal silica particles with average diameters of (A) 12; (B) 22; (C) 45; and (D) 85 nm. Inset: BJH pore size distributions obtained from the corresponding isotherms with maxima at 13, 22, 42, and 90 nm.

droxide, aluminum *iso*-propoxide, water, and ethanol.²⁰ Following the slow evaporation of ethanol from the impregnated CIC at room temperature, tetraethyl orthosilicate (TEOS) was added to the mixture at a CIC/SiO₂ ratio of 2:1 (w/w). The composition of the impregnated synthesis gel on an oxide basis was Al₂O₃/TPAO/Na₂O/SiO₂/H₂O (0.5:9:0.15:50:390). The final mixture was heated in an autoclave at 180 °C for 48 h. The CIC was removed from the composite composition by calcination in air at 570 °C for 8 h. The final nanosized ZSM-5 products were denoted as ZSM-5 (13), ZSM-5 (22), ZSM-5 (42), and ZSM-5 (90), where the number in parentheses indicates the average particle sizes determined from TEM images.

Characterization Methods. X-ray powder diffraction (XRD) patterns were measured on a Rigaku Rotaflex diffractometer equipped with a rotating anode and Cu K α radiation. Transmission electron microscopy (TEM) studies were carried out on a JEOL 100 CX instrument using an electron beam generated by a CeB₆ filament and an acceleration voltage of 120 kV. Samples for TEM studies were prepared by dipping a carbon-coated copper grid into a suspension of samples in ethanol that was pre-sonicated. The nitrogen adsorption–desorption isotherms were measured at –196 °C on a Micromeritics Tristar instrument. Before measurement, samples were evacuated overnight at 250 °C. The BET surface area was calculated from the linear part of the BET plot according to IUPAC recommendations.²⁷ Pore size distributions for CIC carbon samples were calculated from the nitrogen adsorption branch using the BJH model. External surface areas and micropore surface areas for the zeolite samples were estimated from *t*-plots derived from the nitrogen adsorption isotherms.²⁸

Results

Figure 1 illustrates the nitrogen adsorption–desorption isotherms and BJH pore size distribution plots for the four CICs formed through imprinting pitch with colloidal silicas with nominal diameters of 12, 22, 45, and 85 nm according to the method of Li and Jaroniec.²⁵

(20) Schmidt, I.; Madsen, C.; Jacobsen, C. J. H. *Inorg. Chem.* **2000**, *39*, 2279–2283.

(21) Ryoo, R.; Joo, S. H.; Jun, S. J. *Phys. Chem. B* **1999**, *103*, 7743–7746.

(22) Jun, S.; Joo, S. H.; Ryoo, R.; Kruk, M.; Jaroniec, M.; Liu, Z.; Ohshima, T.; Terasaki, O. *J. Am. Chem. Soc.* **2000**, *122*, 10712–10713.

(23) Lee, J.; Yoon, S.; Oh, S. M.; Shin, C. H.; Hyeon, T. *Adv. Mater.* **2000**, *12*, 359–362.

(24) Lee, J.; Sohn, K.; Hyeon, T. *J. Am. Chem. Soc.* **2001**, *123*, 5146–5147.

(25) Li, Z. J.; Jaroniec, M. *J. Am. Chem. Soc.* **2001**, *123*, 9208–9209.

(26) Schuth, F. *Chem. Mater.* **2001**, *13*, 3184–3195.

(27) Sing, K. S. W.; Everett, D. H.; Haul, R. A. W.; Moscou, L.; Pierotti, R. A.; Rouquerol, J.; Siemieniowska, T. *Pure Appl. Chem.* **1985**, *57*, 603–619.

(28) Gregg, S. J.; Sing, K. S. W. *Adsorption, Surface area, and Porosity*; Academic Press: London, 1982.

Table 1. Textural Properties of Colloid-Imprinted Carbon (CIC) Templates

sample ^a	imprinting agent	silica/pitch mass ratio	BET surface area (m ² /g)	total pore volume (cm ³ /g)
CIC-13	Ludox AS-30	1.20	235	0.59
CIC-22	Ludox AS-40	1.60	154	0.55
CIC-42	Snowtex-OL	0.80	71	0.43
CIC-90	Snowtex-ZL	1.60	63	0.65

^a The number in the sample label indicates the average pore size (nm) calculated from the adsorption branch of the nitrogen isotherm.

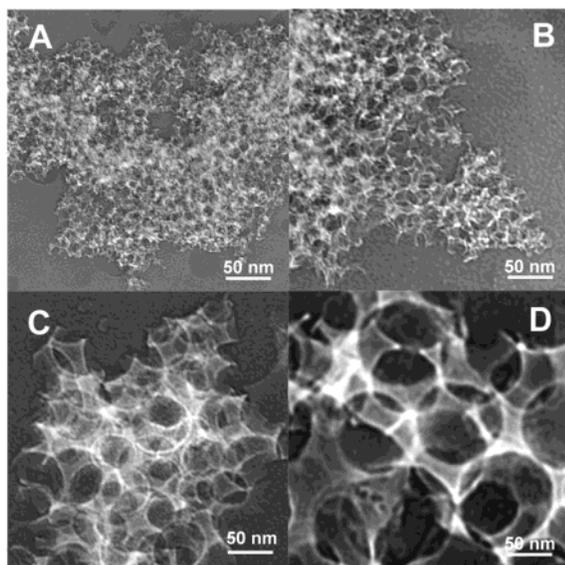


Figure 2. TEM images of CIC carbons (A) CIC-13; (B) CIC-22; (C) CIC-42; and (D) CIC-90 nm. The number in the CIC label is the average pore size (nm) determined from the nitrogen adsorption isotherms in Figure 1.

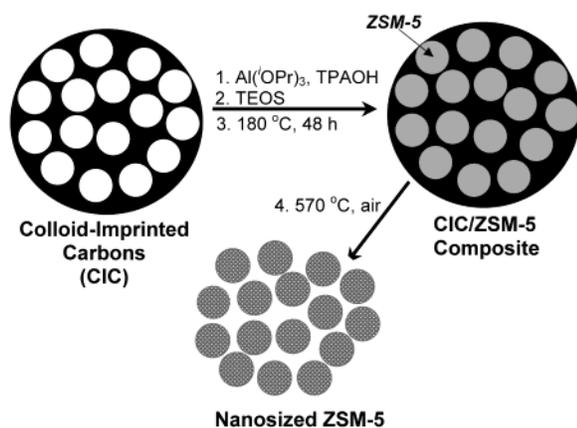


Figure 3. Scheme for the nanocasting synthesis of ZSM-5 zeolite.

The adsorption leg for each CIC exhibits a very sharp nitrogen condensation step indicative of a narrow pore size distribution. The maxima in the BJH pore size distributions occur at 13, 22, 42, and 90 nm, in good agreement with average diameters of the imprinting silica colloids. Also, the imaged pores shown in the transmission electron micrographs in Figure 2, are in agreement with the pore sizes estimated from the adsorption data. The specific BET surface areas and pore volumes for the four CIC templates are provided in Table 1.

As illustrated schematically in Figure 3, the nanocasting of ZSM-5 zeolite was accomplished by first impregnating the CIC pores with a mixture of alumi-

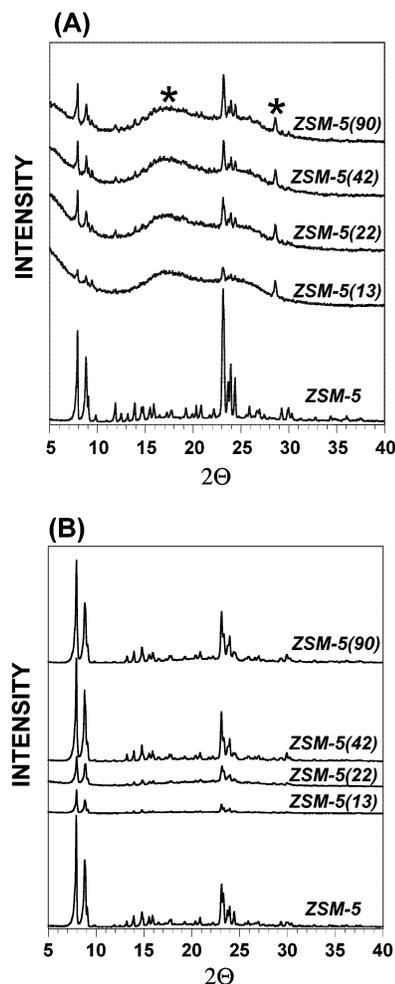


Figure 4. XRD patterns of nanocasted ZSM-5 zeolites: (A) As-made composite compositions prior to the removal of the CIC template and zeolite structure-directing agent and (B) after calcination in air at 570 °C. Included for comparison are the patterns for ZSM-5 made in the absence of a CIC template. The broad peaks in the patterns for the as-made products arise from the CIC template.

num alkoxide as the alumina source and tetrapropylammonium hydroxide (TPAOH) as the zeolite structure-directing agent, followed by impregnation with tetraethyl orthosilicate (TEOS) as the silica source, and digestion of the composite mixture at 180 °C for 48 h.

Figure 4 provides the XRD patterns of the as-made CIC–zeolite nanocomposites, along with the patterns of the nanosized zeolites obtained after removing the CIC by calcination at 570 °C. The diffraction patterns obtained for the as-made nanocomposites are a superposition of the patterns observed for the CIC and the tetrapropylammonium form of the zeolite. All of the reflections found for the calcined nanosized ZSM-5 are attributable to the template-free zeolite.

Table 2. Textural Properties of Nanosized ZSM-5 Crystals Formed through CIC Nanocasting^a

sample	micropore surface area S_{MIC}^b (m ² /g)	external surface area S_{EXT}^b (m ² /g)	BET surface area S_{BET}^c (m ² /g)	S_{EXT}/S_{MIC}	S_{EXT}/S_{BET}	micropore volume (cm ³ /g)	total pore volume cm ³ /g
ZSM-5 (13) ^d	173	127	300	0.73	0.42	0.081	1.27
ZSM-5 (22)	190	59	250	0.31	0.24	0.090	0.65
ZSM-5 (42)	277	33	310	0.12	0.11	0.138	0.36
ZSM-5 (90)	234	21	256	0.09	0.08	0.115	0.30
ZSM-5 ^e	321	16	337	0.05	0.08	0.150	0.20

^a Samples were evacuated overnight at 250 °C. ^b From *t*-plots. ^c From BET. ^d The number in parentheses in the sample label indicates the average particle size (nm) obtained from ten TEM images. ^e This sample was made from the same reagents, but in the absence of a CIC template.

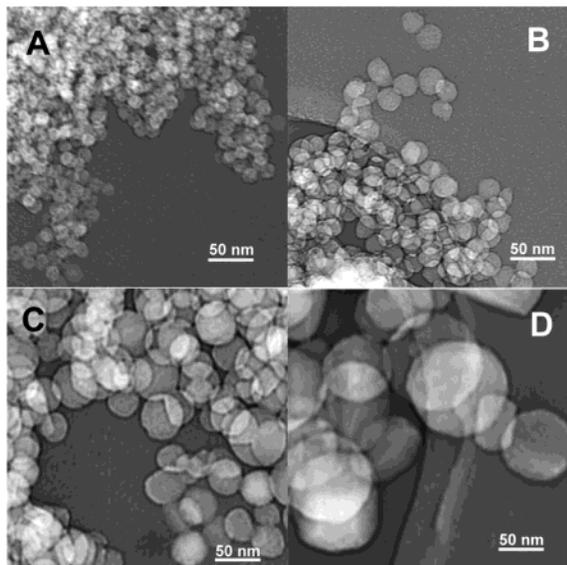


Figure 5. TEM images for calcined forms (570 °C) of ZSM-5: (A) ZSM-5 (13); (B) ZSM-5 (22); (C) ZSM-5 (42); and (D) ZSM-5 (90). The numbers in parentheses are the particles diameters (nm) estimated by averaging the particle sizes observed in ten TEM images.

Figure 5 provides representative TEM images for the ZSM-5 nanoparticles formed through CIC nanocasting. As expected for a nanocasting synthesis process based on CIC templating, the ZSM-5 domains shown in these images are very uniform in size. Most of the nanospheres are intergrown, affording aggregated particles much larger than the fundamental zeolite domain size.

Nitrogen adsorption–desorption isotherms for the ZSM-5 nanoparticles are shown in Figure 6. Included for comparison purposes are the isotherms for ZSM-5 prepared using the same reagents, but crystallized in the absence of a CIC template. Table 2 provides the specific BET surface areas, pore volumes, and related textural properties for the corresponding ZSM-5 samples. To obtain the external surface areas and microporous volumes reported in Table 2, *t*-plots²⁸ were made using the nitrogen adsorption data. Representative *t*-plots are shown in Figure 7 for nanocasted ZSM-5 (13) and for a conventional ZSM-5 made in the absence of a CIC template. The reported micropore volumes and external surface areas were obtained from the intercepts and slopes, respectively, of the best fit of the data between *t* = 0.50 and 0.80 nm, in accord with previously established procedures.^{29–31}

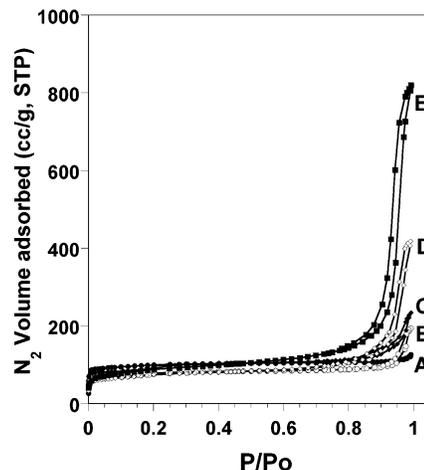


Figure 6. Nitrogen adsorption–desorption isotherms for (A) ZSM-5 made in absence of a CIC template, and for the following CIC-nanocasted forms: (B) ZSM-5 (13); (C) ZSM-5 (22); (D) ZSM-5 (42); and (E) ZSM-5 (90).

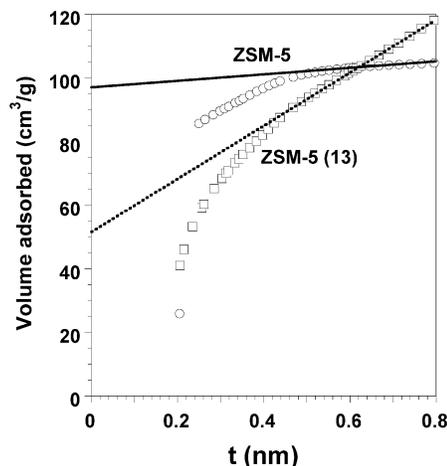


Figure 7. *t*-Plots of the nitrogen isotherms for nanocasted ZSM-5 (13) and conventional ZSM-5 made by the same methodology, but in the absence of a CIC template.

Discussion

The synthesis of CIC materials, as originally reported by Li and Jaroniec,²⁵ used silica colloids with nominal diameters of ~13 and ~24 nm to imprint the pitch precursor. The results of the present work show that colloidal silicas with diameters of ~45 and ~85 nm are also effective in imprinting pitch, at least when the silica to pitch mass ratio is maintained in the region 0.80–

(29) Sing, K. S. W. *Chem. Ind.* **1968**, 2, 1520–1521.

(30) Sayari, A.; Crusson, E.; Kaliaguine, S.; Brown, J. R. *Langmuir* **1991**, 7, 314–317.

(31) Sousa-Aguiar, E. F.; Liebsch, A.; Chaves, B. C.; Costa, A. F. *Microporous Mesoporous Mater.* **1998**, 25, 185–192.

1.60. For each CIC the pore size distribution is uniform and centered near the average diameter of the imprinting colloid. The uniformity of the pore size distributions, as noted previously²⁵ and as reflected in the nitrogen adsorption isotherms and TEM images of the present work (cf., Figures 1 and 2), can be even better than the pore distributions obtained for carbons formed through colloidal crystal replicating methods.^{32,33} As is shown by the insert in Figure 1, silica colloids with a nominal sizes of 12 and 22 nm afford CIC structures with much narrower pore size distributions than the CIC materials imprinted by 45- and 85-nm colloids. These differences in pore size fidelity most likely reflect the variation in the size distribution of the imprinting colloids. Although it is possible to obtain mesoporous carbons with pore size distributions comparable to a CIC by replicating mesostructured silicas,^{21–24} the colloid imprinting of pitch represents a much more convenient and efficient process because it eliminates the need to pre-assemble a metal oxide template. However, carbon replication of silica mesostructures can be expected to be the method of choice when there is a need for forming carbons that are not only mesoporous, but also mesostructured.

The impregnation of a CIC template with a ZSM-5 synthesis gel through incipient wetness methods makes it possible to crystallize the zeolite almost exclusively within the imprinted pores. Essentially all of the zeolite phase is provided in nanodomain form, as verified by TEM (Figure 5). The uniformity of the nanoparticles is correlated with the uniformity of the pores in the initial imprinted carbon template. Most of the nanoparticles formed from CIC templates with average pore sizes of 13 and 22 nm fall in the size range 12–14 and 25–28, as determined by TEM. The distribution of particle sizes obtained from the 42- and 90-nm CIC templates was broader, namely, 32–45 and 70–100 nm, respectively. Thus, the crystallite sizes for CIC-nanocasted forms of ZSM-5 are substantially more uniform than those obtained previously though the use of carbon black as a nanocasting template.²⁰ Carbon blacks with nominal pore sizes of 32 and 46 nm have been reported to yield

ZSM-5 nanoparticles of 22–30 and 37–45 nm, respectively, so that neither the size nor the shape of those particles was nearly as uniform as those obtained in the present work.

The size and shape fidelity of CIC-nanocasted ZSM-5 allows one to control both the external surface area (16–127 m²/g) and the interparticle mesopore volume (0.05–1.19 cm³/g) through a rational choice of the template pore size (cf., Table 2). This flexibility in tailoring the particle textural properties makes it possible to optimize the catalytic properties of the zeolite for the conversions of molecules that are too large to penetrate the framework micropores and constrained to reacting only at active sites on the external particle surfaces. Conversely, for small molecule conversions within the framework micropores, nanocasting also makes it possible to tailor uniformly the diffusion path length to optimize reactivity or selectivity. Thus, nanocasting is a versatile alternative to the templating of hollow spheres of zeolite particles^{34–36} as a means of introducing mesoporosity.

The zeolite nanoparticles obtained though CIC nanocasting are intergrown into larger aggregates, reflecting the pore connectivity of the templating CIC. Such aggregates are desirable for catalytic applications because they afford free-flowing powders that can be processed with retention of the desired nanoscale domain size, but without creating a serious dust nuisance. The powders can also be processed in aqueous suspension, if desired, and recovered by filtration without the loss of the nanoparticles. Thus, CIC-nanocasting affords a zeolite phase that combines the catalytic advantages of a colloidal zeolite particle while retaining the processing advantages of a conventional zeolite.

Acknowledgment. The funding of this research though NSF grant CHE-0211029 and though NIEHS grant ES04911 in support of S.S.K. is gratefully acknowledged.

CM021762R

(32) Zakhidov, A. A.; Baughman, R. H.; Iqbal, Z.; Cui, C. X.; Khayrullin, I.; Dantas, S. O.; Marti, I.; Ralchenko, V. G. *Science* **1998**, *282*, 897–901.

(33) Yu, J. S.; Yoon, S. B.; Chai, G. S. *Carbon* **2001**, *39*, 1442–1446.

(34) Kulak, A.; Lee, Y.-J.; Park, Y.-S.; Kim, H. S.; Lee, G. S.; Yoon, K. B. *Adv. Mater.* **2002**, *14*, 526–529.

(35) Dong, A.; Wand, Y.; Tang, Y.; Ren, N.; Zhang, Y.; Gao, Z. *Chem. Mater.* **2002**, *14*, 3217–3219.

(36) Valtchev, V. *Chem. Mater.* **2002**, *14*, 4371–4377.